NASA SP-8042

SPACE VEHICLE
DESIGN CRITERIA
(STRUCTURES)

METEOROID DAMAGE ASSESSMENT

MAY 1970

NATIONAL AERONAUTICS AND SPACE ADMINISTRATION

FOREWORD

NASA experience has indicated a need for uniform criteria for the design of space vehicles. Accordingly, criteria are being developed in the following areas of technology:

Environment
Structures
Guidance and Control
Chemical Propulsion

Individual components of this work will be issued as separate monographs as soon as they are completed. A list of all previously issued monographs in this series can be found at the end of this document.

These monographs are to be regarded as guides to design and not as NASA requirements, except as may be specified in formal project specifications. It is expected, however, that the criteria sections of these documents, revised as experience may indicate to be desirable, eventually will become uniform design requirements for NASA space vehicles.

This monograph was prepared under the cognizance of the Langley Research Center. The Task Manager was T. L. Coleman. The author was V. C. Frost of Aerospace Corporation. A number of other individuals assisted in developing the material and reviewing the drafts. In particular, the significant contributions made by P. C. Chou of Drexel Institute of Technology; R. J. Eichelberger of U. S. Army Ballistic Research Laboratory; J. Erickson of The Boeing Company; J. W. Gehring and C. J. Maiden of General Motors Corporation; E. T. Kruszewski of NASA Langley Research Center; L. Long of Lockheed Missiles & Space Company; A. J. Richardson of North American Rockwell Corporation; M. V. Scherb of McDonnell Douglas Corporation; A. Schreeves of Grumman Aircraft Engineering Corporation; J. D. Stewart of General Electric Company; and J. H. Tillotson of Edgerton, Germeshausen and Grier, Incorporated, are hereby acknowledged.

May 1970

CONTENTS

METEOROID DAMAGE ASSESSMENT

1. INTRODUCTION

The impact of a meteoroid on a space vehicle can damage the flight-critical systems of the vehicle and jeopardize its flightworthiness. The term "meteoroid" is used here in its broadest sense to include lunar ejecta as well as particles of cometary and asteroidal origin. Meteoroid impact can cause partial penetration, perforation, spall, local deformation, or secondary fractures, any of which can result in failure of the vehicle's critical systems. Such failure commonly takes one or more of the following forms:

- Catastrophic rupture.
- Leakage.
- Deflagration.
- Vaporific flash.
- Reduced structural strength.
- Erosion.

The ability of meteoroids to penetrate the external skin of a spacecraft has been amply demonstrated by meteoroid-detection satellites such as Explorers XVI and XXIII, and by the three Pegasus vehicles.

This monograph presents a discussion of procedures for determining meteoroid damage to and providing protection for the structure of space vehicles. Subsystems such as nonintegral tanks and thermal protection systems for entry vehicles are considered, as well as the principal load-carrying elements. However, damage to mechanical or electrical components is not discussed, and injury to the crew is considered only indirectly.

The meteoroid characteristics applicable to vehicle design are customarily specified in the form of a model of the meteoroid environment. A recent model, published in a

NASA monograph (ref. 1), covers the near-earth, cis-lunar, and near-lunar environments. A model environment for meteoroids encountered in interplanetary space, and particularly in the asteroidal belt between Mars and Jupiter, will be presented in a planned NASA monograph.

Because the major portion of the meteoroid flux has a random distribution, a statistical model is used to determine the probability of encountering a meteoroid with a mass equal to or greater than a given mass. For any particular probability, the design value of meteoroid mass is a function of the size of the exposed structural area and the exposure time. The design value of meteoroid velocity is commonly based on an average value, but a probability distribution may also be used. It is customary to use an average value of meteoroid density, and the angle of impact is frequently assumed normal to the surface of the structure.

The damage capability of a meteoroid depends on its mass, velocity, density, and angle of impact. The shape of the meteoroid and its orientation relative to its trajectory can also affect the degree of the damage, but present knowledge of the meteoroid environment is inadequate to specify these parameters. It is therefore customary to assume that the meteoroid has a compact shape (i.e., a shape of approximately equal major dimensions).

The physical response of any structure under meteoroid impact depends on the material, temperature, stress level, thickness, number, and spacing of the plates composing the structure. The degree of damage is determined by analytical methods and tests.

The requirements for meteoroid protection are of direct interest to designers of several space-vehicle systems. Among the most significant are the radiation protection system, the thermal protection system, thermal insulation, and space radiators, when incorporated with the structure.

2. STATE OF THE ART

Current knowledge of meteoroid damage has been acquired through numerous experimental and theoretical investigations, but in spite of these extensive efforts the technology remains inadequately developed. Moreover, the investigations have sometimes produced conflicting conclusions which have led to an imperfect understanding of the existing technology. It is therefore necessary to recognize the limitations of existing techniques and to recognize the types of damage applicable to various structures.

A methodology for the prediction of meteoroid damage must provide for a range of velocity from less than 1 km/sec to 72 km/sec, and for any angle of impact. The method must also be valid for meteoroids varying from porous, highly frangible particles with a density of 0.5 g/cc to solid particles with a maximum density of 8.0 g/cc. Analytical methods are available only for fairly simple structures. For more complex structures, methods and tests must be devised.

For purposes of this monograph, the velocity range for meteoroid impacts is divided into low, intermediate, and hypervelocity regimes. These regimes are distinguished by differences in the physical response of the various types of structure, as described in Section 2.3, rather than by the actual magnitude of the velocity.

2.1 Experimental Techniques

The customary means of evaluating the degree of resistance of most structures to meteoroid damage is by experiment. Most of the experimental data suitable for engineering purposes have been obtained by using particle accelerators that project a small pellet at a target simulating a particular structure. The pellet must remain intact until impact, and the mass and velocity of the pellet must be controllable and accurately measured. It would also be desirable to simulate the entire range of meteoroid parameters, but no existing accelerator has this capability.

Ideally, the pellet material should duplicate the density and composition of the meteoroid. However, since the pellet must remain intact until impact, exact simulation of frangible, low-density cometary meteoroids is not practical. In the past, aluminum and glass have been the materials most frequently used as pellets, and they are still generally considered a reasonable and convenient compromise. Syntactic foam, a material composed of minute hollow glass spheres in a plastic matrix, has also performed satisfactorily with a density as low as 0.7 g/cc.

Experimental techniques differ in the type of particle accelerator used. Each type has certain limitations which affect its suitability for any specific test.

2.1.1 Light-Gas Guns

The light-gas gun is by far the most frequently used accelerator. This gun has a distinguishing feature of accelerating the projectile by using the pressure of an expanding light gas (e.g., helium or hydrogen). The projectile usually consists of two components: a pellet that simulates the meteoroid and a sabot that supports the pellet. The sabot is diverted just beyond the muzzle of the gun and does not impact the target. Detailed information on types of light-gas guns and on the mechanics of their operation is provided in references 2 and 3.

The light-gas gun accelerates an intact pellet of known mass and allows the best simulation of the desired range of meteoroid density. Another important advantage of this type of accelerator is that the velocity can be determined accurately and is readily controllable. For many actual structures, the light-gas gun is the only particle accelerator that consistently produces usable data.

The principal limitation of the light-gas gun is that its maximum velocity is far less than the velocity of meteoroids. Although velocities as high as 11 km/sec have been achieved with the light-gas gun (ref. 4), the usual test is limited to approximately 7 to 8 km/sec. However, explosive light-gas guns now being developed offer the potential of higher velocities (ref. 5).

2.1.2 Other Particle Accelerators

Several other types of particle accelerators are listed in table I with their approximate capabilities and limitations indicated. Some of these accelerators provide a velocity substantially higher than the velocity obtained with light-gas guns, but only at the

TABLE I. – CHARACTERISTICS OF OTHER PARTICLE ACCELERATORS

Type	Reference no.	Capability	Comment no.
Electric-arc lithium plasma	6	Typical velocities 12 to 14 km/sec with particle mass from 10^{-8} to 10^{-6} g. Maximum velocity, 20 km/sec.	1, 2, 3
Electrostatic	7	30 km/sec with submicron-size iron particle. Higher velocities potentially possible.	1, 3
Exploding foil	8, 9	8 km/sec with particle mass of a few milligrams.	4, 5
Hotshot tunnel	10	30 km/sec with particle mass of approximately 6×10^{-8} g.	1, 3, 4, 6
Shock tube	11	Potential velocity of approximately 9 km/sec with multiple particles 1 to 4 μ in size.	1, 3, 4, 6

Comments

1. Unsuitable for penetration tests of most actual structures because of small mass of particle.
2. Particularly suitable for penetration-mechanics research on simple targets.
3. Can launch multiple particles; has possible application for meteoroid-erosion tests.
4. Difficult to control and determine the particle parameters.
5. Possible particle breakup.
6. Possible particle ablation.

expense of greatly reduced particle mass. These accelerators are not suitable for penetration tests of most actual structures because they would require extensively scaled-down models of the structure. Scaling would be an extremely dubious procedure, because of the present state of the art. However, those accelerators for which the particle mass and velocity can be determined accurately may be suitable for penetration-mechanics research and/or meteoroid-erosion tests.

2.2 Theoretical Techniques

Because of the velocity limitations of experimental techniques, theoretical methods have been developed to predict meteoroid damage in the hypervelocity range. Some of these methods are of substantial value as a research tool and can be used in the design of some types of structure. Hydrodynamic theory has been used extensively for hypervelocity impact of a solid or porous projectile on a semiinfinite body [i.e., a body whose dimensions are large with respect to those of the crater (refs. 12 to 14)].

Single thin plates have also been investigated (refs. 13 to 15). In recent years the hydrodynamic technique has been extended to include material-strength effects. This modified theory has been applied to the semiinfinite body (refs. 16 and 17), to a single thin plate (ref. 18), and to two spaced plates (ref. 19).

The hydrodynamic method provides an excellent understanding of the physical aspects of the penetration process, and particularly of the mass flow, pressure distribution, and velocity field of the spray of material emerging from the aft face (ref. 18). In some cases, it has also made possible the establishment of useful scaling relations. However, the interaction of a projectile with a spacecraft structure frequently involves several types of damage, and even the most advanced existing hydrodynamic/strength methods do not accommodate all possible combinations of damage.

In the application of the hydrodynamic method, the equations of time-dependent, compressible, hydrodynamic flow are solved by numerical techniques, using large high-speed computers. The maximum size of the problem is currently limited to the two-dimensional case, (e.g., an axisymmetric projectile impacting normal to the surface of the plate). For impact at an angle, an approximation must be used (ref. 20). However, three-dimensional solutions now under development should accommodate oblique impact directly.

A technique for determining the ballistic limit of two spaced plates subject to hypervelocity impact is provided in reference 21. In this method, the momentum distribution and the density-velocity profiles of the ejecta from the first plate are determined by hydrodynamic theory. The impulse loads from the ejecta are applied to

the second plate, and the large-deformation dynamic response of the plate is calculated, including both elastic and plastic effects. This method can be used to determine initial spall fracture, but it does not determine whether detached spall fragments will occur, nor does it account for the effect of discrete solid particles in the ejecta. A somewhat simpler but more approximate technique is also available (ref. 22). In this method, the distribution of the ejecta mass and velocity is assumed and the second plate is analyzed by linear elastic small-deflection plate theory.

An analytical solution is also available for determining the threshold of perforation of a single thin plate (ref. 23). This method is based on viscoplastic-flow theory and includes the effect of the material's yield strength. There is some controversy, however, as to whether the physical model of the perforation process is entirely realistic at hypervelocity.

2.3 Damage Modes

Data on various types or modes of damage to spacecraft structure have been obtained from numerous tests. Most of the tests, however, have been concerned with simple ductile metal targets at room temperature. The projectiles have usually been solid compact metal or glass pellets, and the impacts have usually been normal to the surface of the target. These limitations reduce the general applicability of the test data, and caution must be exercised in their interpretation.

Damage modes of structural significance are:

- Partial penetration and/or surface damage.
- Perforation.
- Local deformation, spall fracture, or detached spall at the back surface.
- Secondary fracture.
- Catastrophic rupture.

There is a distinction between damage and failure. Several types of failure can result from certain types of damage. For example, both vaporific flash and leakage can be caused by perforation of the wall of a pressure cabin. Conversely, a damage mode may be synonymous with failure, as in a catastrophic rupture. The relationship of the damage modes to the various types of structural failure is considered in Section 4.

2.3.1 Semiinfinite Body

In a semiinfinite body, the lateral and thickness dimensions are large with respect to the dimensions of the impact crater. Many of the theoretical and experimental investigations conducted to date have been concerned with this type of structure because of its basic simplicity. A considerable amount of useful data has been gathered and quantitative relationships established. These relationships serve as a convenient means of examining the influence of the various parameters and help provide an understanding of the effect of meteoroid impact on single-plate targets. However, direct extrapolation of semiinfinite body data to more sophisticated targets can lead to erroneous conclusions.

In a semiinfinite body, the significant damage is limited to the depth of crater and to the extent the surface area is destroyed. Solid compact projectiles in the low-velocity regime form a deep, narrow, cylindrical crater, primarily by mechanical deformation. In the hypervelocity regime, enormous shock pressures are created at the interface between the projectile and plate. As the shock passes through the plate, the material is compressed almost instantaneously to an extremely high pressure. After passage of the shock, the pressure decreases rapidly and the material expands adiabatically. Irreversible heating of the plate material occurs during this process, with the amount of heat depending on the strength of the shock. Extensive recrystallization of the material adjacent to the crater can be caused by large shocks.

As the shock passes through the plate, its intensity is reduced by spherical divergence and rarefaction waves reflected from the free surfaces. The pressure eventually becomes comparable with the strength of the material, and growth of the crater is arrested. The resulting crater is nearly hemispherical. In the intermediate velocity regime the crater shape changes from cylindrical to hemispherical (refs. 24 and 25).

2.3.1.1 Effect of Projectile Density

It has been demonstrated by experiment that the density of the projectile material influences the crater dimensions, but that the magnitude of this effect diminishes with increasing velocity. The near-hemispherical crater typical of the hypervelocity regime is associated with projectiles of the same density as the plate material. For projectiles of appreciably lesser density, the crater tends to become broad and shallow rather than hemispherical, and for those of greater density, it becomes deeper (ref. 25).

It has also been shown theoretically that the density effect on the crater depth persists at least to some small degree at the higher meteoroid velocities. This effect appears to be linked with the lower shock pressures induced by porous projectiles (ref. 12).

2.3.1.2 Effect of Projectile Diameter

A diameter-scaling effect is reported in reference 26 for 2024 aluminum alloy. In this experimental investigation, it was discovered that the crater depth scaled as the 19/18ths power of the diameter of a spherical projectile. The crater diameter was also affected, but to a slightly different degree. This effect was demonstrated over a diameter range of four orders of magnitude.

2.3.1.3 Effect of Impact Angle

The physical effects of the angle of impact of a projectile on the nature of the crater vary with velocity. In the low-velocity regime, the axis of the cylindrical crater formed tends to coincide with the velocity vector for substantial angles relative to the target surface. The projectile ricochets at very small angles, leaving a shallow elongated gouge in the surface. For impact at a constant velocity in the hypervelocity regime, the crater is nearly hemispherical down to some limiting angle, below which the crater becomes asymmetrical. The value of the limiting angle seems to depend on target material and impact velocity. Although the major portion of the projectile mass will be deflected at extremely small angles of impact, it appears that this tendency is less in the hypervelocity regime than in the low-velocity regime.

In the low-velocity regime, the depth penetrated normal to the surface usually correlates with a function of the normal component of velocity, although the minimum angle for which this correlation is valid is not known. Similarly, in the hypervelocity regime, the crater depth can be correlated directly with the normal component of velocity for impact angles down to about 30 degrees. For smaller values of impact angle, the crater depth is less than the predicted value based on the normal component. In addition, the limiting value of the minimum angle appears to decrease with increasing velocity (refs. 24 and 25). For a semiinfinite body, it is frequently assumed that all meteoroid impacts are normal to the surface. This assumption is conservative for the crater depth, but the extent of surface area destroyed may be underestimated. More specific information is not available.

2.3.1.4 Effect of Target Characteristics

The physical characteristics of the body known to affect the crater dimensions significantly are strength, density, ductility, and temperature. It has been shown in experiments that the effect of material strength is appreciable at low velocity, and in theory it is still of some significance at hypervelocity. In the latter case, the strength is obviously significant during the terminal phase of crater formation, at which time the pressure is comparable with the material strength (refs. 26 and 27). A number of

attempts have been made to determine an appropriate strength parameter for inclusion in an expression for crater dimensions. Yield and ultimate-tensile strength, ultimate-shear strength, and Brinell hardness number have been the strength terms most commonly proposed. However, only limited agreement with experiment has been achieved with these parameters (ref. 28).

The density of the target material appears in several expressions for the hypervelocity crater dimensions, and it seems reasonable that the density would influence the inertia forces during fluid flow. This density effect is frequently expressed as the inverse one-half power, but this form is not universally accepted.

The ductility of the material has a pronounced influence on the nature of the crater, particularly at the higher velocities. In a highly ductile material, the crater characteristically has a raised lip, while for less ductile materials this lip is often removed by a fracture occurring slightly below the original surface. With further decreases in ductility, the interior surface of the crater becomes pitted as a result of local spall, and minute cracks appear. For brittle materials, this spalling may become so extensive that the normal crater shape is completely obscured.

The temperature range for spacecraft extends from cryogenic to substantially elevated values. The strength and ductility of the target material are affected by these temperatures, with the result that changes occur in the nature and dimensions of the crater. At elevated temperatures, crater dimensions are increased, and any tendency of the crater surface to spall is reduced. At cryogenic temperatures, the tendency to spall is increased and a more pronounced irregularity occurs in the crater shape. Attempts have been made to correlate the crater dimensions with the physical properties at elevated temperatures, but no general agreement has been reached as to the most appropriate method (ref. 29).

2.3.2 Single Thin Plates

As defined here, the term "thin plate" means that the thickness is limited to a small multiple of the crater dimensions, and no limitation on the absolute thickness is implied. Such plates are typical of a considerable portion of many spacecraft structures. The damage modes of interest are described in the following paragraphs.

When a thin, ductile, metal plate is perforated by a solid, compact projectile at low-impact velocities, a plug of approximately the same diameter as the projectile is punched out. An approximately cylindrical rough-edged hole results.

When the thickness of the plate is large, relative to the crater dimensions, and the impact is in the hypervelocity regime, the crater is similar to that formed in a

semiinfinite body, and the aft surface of the plate may not be affected. As the plate thickness is decreased or the velocity increased, the depth of the crater increases and its shape becomes elongated.

At some value of reduced thickness, a bulge usually appears on the aft face, accompanied by one or more fractures in planes parallel and adjacent to the aft face. This condition is defined as partial penetration with incipient spall. As the plate thickness is reduced further, this bulge increases in size and the internal fractures increase in number and severity. Fragments of this disturbed material may break away from the aft face of the parent plate with an appreciable velocity. These fragments are referred to as detached spall, and the condition as spall threshold.

With further reductions in the plate thickness, the depth of the crater and the intensity and extent of the spall continue to increase. The material remaining between the crater and spalled area becomes excessively deformed, and cracks can occur through the material. When the crater and spalled region extend completely through the plate, the hole has the approximate shape of an hourglass. As the thickness is reduced further, the constriction in the hole diameter decreases until finally the hole becomes approximately cylindrical. The various degrees of cratering and spall are illustrated in figure 1, and the changes in hole diameter are shown in figure 2.

The plate thickness at which threshold penetration or ballistic limit occurs has been defined by various criteria in the experiments conducted to date. These criteria include the capability of the plate to sustain a pressure differential after impact, the ability of a dye to penetrate the impacted plate, and the ability to see light through the plate. The threshold-penetration thickness depends on which criterion is used; for example, the pressure-differential criterion results in larger thicknesses than does the light-transmission criterion.

In general, the influence of the projectile and plate parameters on the hole or crater is similar to that for a semiinfinite body. For perforation in the hypervelocity regime, the relation of hole area to angle of impact may be an exception. Some experimental data have shown that as the angle is reduced, the hole becomes more oval, and that the maximum hole area occurs at an intermediate angle. There are also indications that at this angle the variation of the hole area with velocity may be significantly different from the variation with normal impact (refs. 30 and 31).

An additional parameter for thin plates is a stress field. Impact of a projectile on a stressed plate can cause catastrophic cracking. Moreover, this type of damage can occur even when the crater caused by the projectile does not extend completely through the plate. It has been demonstrated experimentally that for a given material the possibility

t = 10.2 mm
p = hole

t = 12.7 mm
p = 7.12 mm

t = 14.2 mm
p = 6.86 mm

t = semi-infinite
p = 6.61 mm

NOTES

2024-T3 aluminum targets

3.2-mm diameter spherical aluminum projectiles

7.4 km/sec projectile velocity

t = target thickness
p = depth of penetration

Reproduced by permission of General Motors Defense Research Laboratories

Figure 1. – Effect of thickness on depth of penetration and spall.

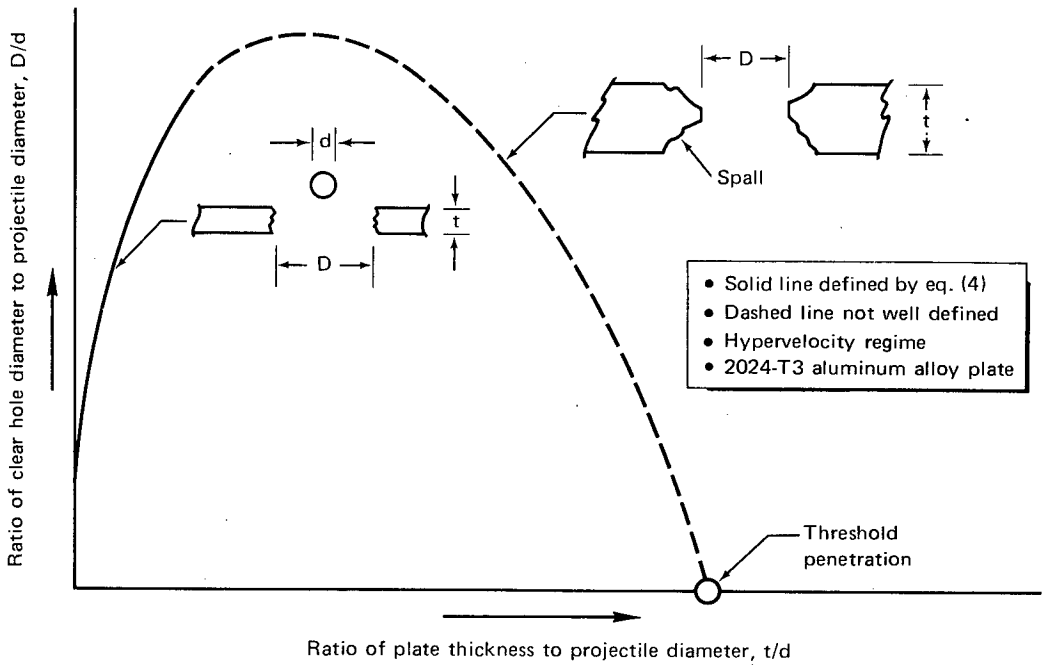

Figure 2. – Schematic description of how shape of hole varies with plate thickness at constant impact velocity.

of such damage is a function of the level of the stress field and of the degree of initial damage from the impact. This initial damage can be measured in terms of hole diameter, initial crack length, or a local reduction in thickness. Quantitative experimental data that relate stress level to degree of damage are reported in reference 32 for several structural materials. It is important to note that this reference shows that the failure stress for a specimen impacted under load is less than the stress for a specimen with the same degree of damage, but loaded after impact. It also appears that a stress field does not affect the impact-crater dimensions nor the hole diameter in the case of perforation.

Brittle materials are particularly sensitive to the reflection of the impact-induced shock wave from any free surface or discontinuity. In addition to spall, severe cracking can occur through the thickness of the plate. These cracks generally extend from the edges of the plate and from the impact crater. The extent of these secondary fractures is influenced by the material, size, and shape of the plate, and by any materials in contact with the free surfaces. A comprehensive description of this phenomenon is given in reference 33. The degree of damage can be greatly increased by these secondary fractures. Beryllium, glass, and graphite are particularly susceptible, but quantitative data are almost entirely lacking. Some qualitative experimental data are available however (refs. 33 to 36).

2.3.3 Multiplate Structure

A multiplate structure is defined as a series of spaced plates. The thickness, spacing, and material of the individual plates may vary, and in some instances the intervening spaces may contain an energy-absorbing medium. This type of structure is used for much of the area of the exterior walls of manned spacecraft, and particularly for the pressurized cabin. Practical considerations generally limit such walls to two or three plates.

While both theoretical and experimental studies have been made of multiplate structures, the complexity of these structures has limited the amount of significant data developed. Existing knowledge of the response of these structures is based largely on experiments involving solid, compact metal or glass projectiles and ductile metal plates. The following discussion is limited by these circumstances, and is primarily concerned with two-plate structure.

The first plate in a multiplate structure is designated as the bumper or shield. The function of the shield is to break up the projectile, disperse the fragments, and reduce their velocity below that of the original projectile. Damage to the second plate is caused by the debris from the projectile and shield. The condition of this debris determines the extent and type of damage to the second plate.

2.3.3.1 Characteristics of Debris and Resultant Damage

For normal impact at low velocity, a solid, compact metal projectile will remain intact while penetrating both the shield and second plate. The hole in the second plate will be regular in shape and can be slightly larger than the projectile. With a slight increase in velocity, the projectile will fracture during perforation of the shield. The debris will consist of a tight cluster of relatively large fragments of the projectile and shield. The damage to the second plate will be limited to a single crater or a sheared hole.

At intermediate velocities, the spray of debris will be in the shape of an elongated bubble, and will consist of small solid particles. The size and lateral dispersion of these particles depend on the impact velocity and, to a lesser extent, on the thickness of the shield. The size of the particles will decrease and the lateral dispersion will increase with increased velocity. Both tend to increase with increased shield thickness.

Damage to the second plate can be in the form of a broad, shallow crater composed of a number of overlapping particle craters. If the impact of the debris is severe, it will result in a rough, irregular hole in the second plate. If the plate spacing is increased sufficiently, scattered separate craters or holes will occur because of the individual particles.

As the velocity is increased further into the hypervelocity regime, the particle size will continue to decrease and its physical characteristics will change. The debris will be in the form of unusually small solid particles and minute drops of melted metal. At extremely high velocities, much of the debris can be vaporized. The ability of this debris to form craters in the second plate will be limited to a slight roughening of the surface. The debris will act as an impulse load on the second plate, and cause it to bulge locally. As this bulge becomes more severe, a tension failure will occur, radial cracks will form, and the material between the cracks will be bent back by the pressure. The resulting hole will usually have a petalled appearance. If the pressure pulse is sufficiently intense, the petals will break off at the root, and an irregularly shaped, rough-edged hole will result (ref. 21). The variation of the debris with velocity is illustrated in figure 3 and the resultant damage indicated in figure 4.

In the hypervelocity regime, the second plate may also be damaged by fragment impact. The last few bits of material removed from the shield tend to be solid particles that are larger and slower than those contributing to the impulse load. These "late" fragments can cause small, scattered, individual craters or holes in the second plate adjacent to the outer edge of the impulse-loaded area. These late fragments have been observed at velocities of approximately 8 km/sec, and it is believed that they can occur at higher meteoroid velocities. The degree of interaction between the damage caused by the late fragments and the damage from the impulse load is poorly defined. However, significant scatter in threshold penetration is possible as a result of these combined effects (ref. 32).

For oblique impact, a significant change occurs in the debris. One group of particles follows closely the original trajectory, while the path of the other group is normal to the shield. The normal group is dispersed laterally, and appears to consist primarily of particles from the shield. These particles are larger and slower than those for a normal impact at the same velocity. The other group appears to consist largely of projectile particles and is less dispersed. Either or both groups may penetrate the second plate (refs. 21 and 37).

At the higher velocities, the back face of the second plate may spall, regardless of the condition of the debris. The spall depends only on the magnitude of the impulse load and on the material and thickness of the plate. It should be noted that spall can occur even when the second plate is not perforated. The characteristics of this spall are similar to those for a single thin plate.

Interaction of impact damage with a stress field can cause catastrophic cracking of the second plate in the same manner as for a single thin plate. Since the lateral extent of the damage is greater than that in a single plate, the second plate is more susceptible to this type of failure. It has been demonstrated that a single-stressed plate that did not

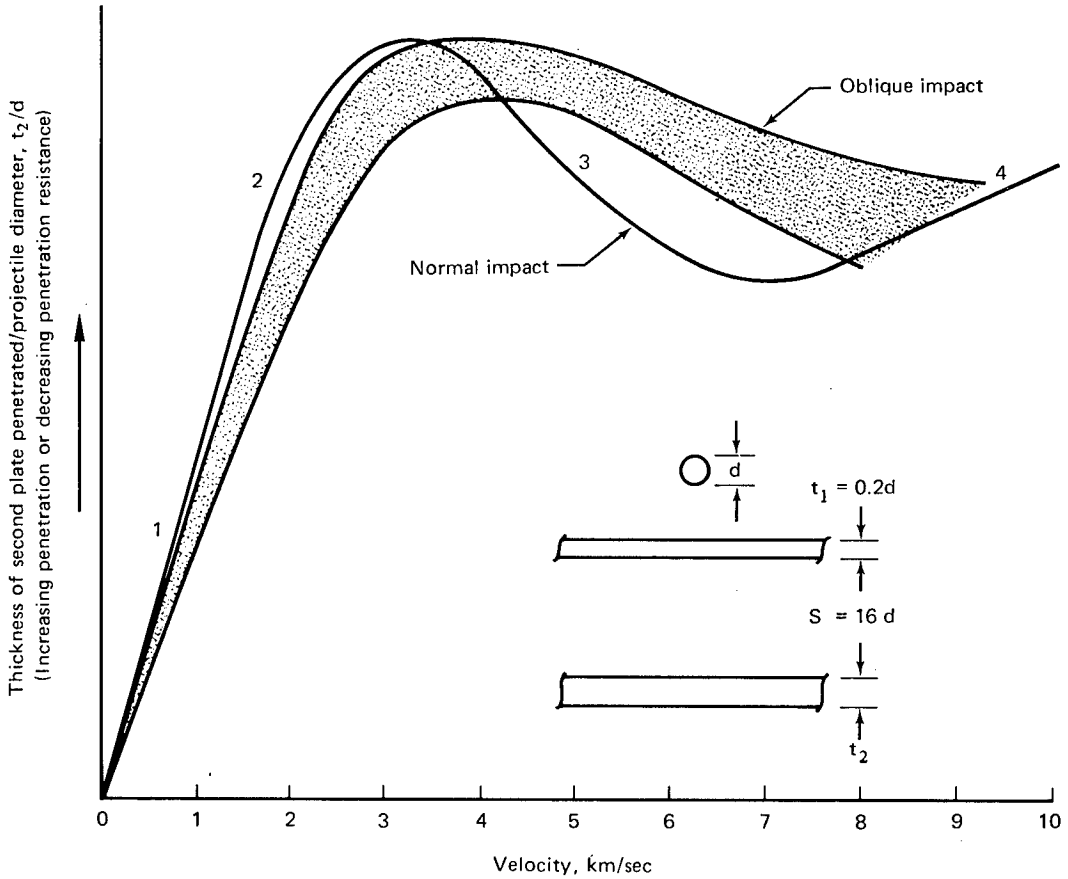

Notes:

Numbers on normal impact curve show the variation of debris with velocity

1. Intact projectile.
2. Tight cluster of relatively large fragments of projectile and shield.
3. Debris in shape of elongated bubble with surface composed of numerous small solid particles of projectile and shield.
4. Debris consisting of:
   A. Elongated bubble composed of very small solid particles, minute drops of melted metal, and metal vapor.
   B. A few solid fragments which are larger and slower than the balance of debris.

Figure 3. – Schematic description of how penetration resistance and debris vary with velocity (aluminum projectiles on aluminum alloy structure).

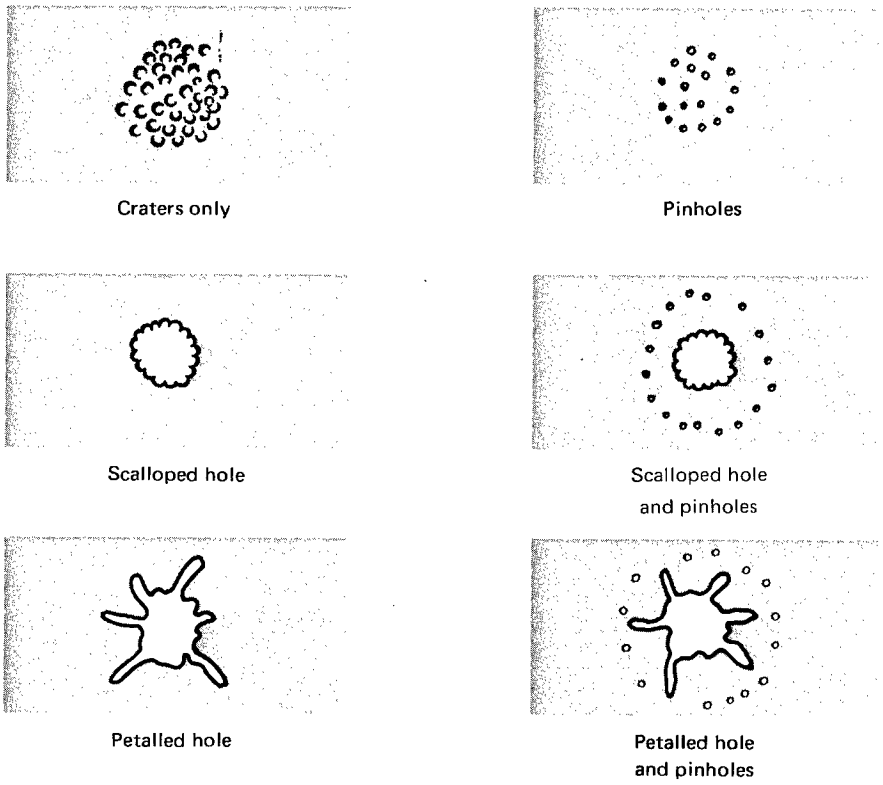

Reproduced by permission of The Boeing Co.

Figure 4. – Damage patterns on second plate of multiplate structure.

fail under impact can fail catastrophically under the same conditions by the addition of a shield (ref. 32). Perforation of the second plate is not necessary for catastrophic cracking.

The density of the meteoroid is expected to affect the degree and type of damage experienced by a two-plate structure. Experiments with low-density projectiles, notably syntactic foam, have shown that the damage to the second plate from impulse loads is slightly less than that produced by aluminum projectiles of equal mass. However, the fragment-impact damage to the second plate increases, presumably because of the smaller impact shock generated (ref. 21).

For three spaced plates, the condition of the debris impacting the third plate is poorly defined. At the higher test velocities, the damage appears to result from solid, high-velocity fragments from the preceding plates. The resulting damage modes can take any form that is characteristic of the second plate (refs. 32 and 38).

2.3.3.2 Resistance to Penetration

For an aluminum projectile and two spaced aluminum alloy plates, the variation of penetration resistance with velocity is illustrated in figure 3. It should be noted that as a result of the changes in the characteristics of the debris, a low-velocity peak occurs. At velocities below the peak, the penetration resistance will be slightly less than for a single plate with the same total thickness.

The thickness of plates penetrated will usually be affected by impact at oblique angles. As shown in figure 3, there is somewhat less penetration from impact at an oblique angle than from normal impact at velocities less than 3 km/sec. At velocities from 3 to 8 km/sec, an increase in penetration will occur for all impacts except those at very small angles. However, this penetration will not exceed the low-velocity peak for normal impact. At hypervelocity, it is anticipated that the impulse load will be reduced and that the late fragment damage will not be much different than for normal impact. Therefore, if a two-plate structure is capable of resisting penetration from normal impact over the velocity range, it will be adequate for oblique impact (ref. 21).

For two spaced plates, the resistance to penetration varies with spacing, with the degree of variation depending on the characteristics of the debris, and consequently on the velocity (refs. 21 and 32). Spacing has little effect on the plates' resistance to penetration at low velocities because the debris is limited to a small number of large fragments. In the intermediate-velocity regime, increased spacing allows the debris to impinge on the second plate over a larger area. Consequently, the resistance to penetration increases with spacing up to the point at which scattered individual craters occur. There is also a lower limit for the spacing, below which the resistance decreases rapidly. For an aluminum projectile and aluminum alloy plates, this lower limit occurs at a spacing of approximately eight projectile diameters (ref. 29).

In the hypervelocity regime, the required thickness of the second plate to resist failure under an impulse load varies inversely with the square of the spacing (refs. 21 and 22). For the late fragments, however, the spacing is ineffective in increasing the penetration resistance.

The results of theoretical and experimental study of the effects of shield thickness on fragment-impact damage to a semiinfinite body are reported in reference 38. For an aluminum projectile and shield, it was determined that the total penetration was a minimum for a ratio of t_1/d of 0.15 at a velocity of 8 km/sec. For values of t_1/d from 0.15 to 0.50, the total penetration increased slightly, but for values less than 0.1, the penetration increased rapidly. It was also found that the value of the optimum ratio decreased with increasing velocity over the range considered.

Limited investigations have been made of the influence of shield thickness relative to projectile diameter (t_1/d) on the combined fragment-impact and impulse-load damage to thin second plates (refs. 21 and 39). For aluminum projectiles and two-plate structure, it was determined that at a velocity of approximately 7 km/sec, the combined thickness of the first and second plates was a minimum at a value of t_1/d in the region of 0.25. For higher values of t_1/d, the total thickness increased in a roughly linear manner. The thickness of the second plate alone, however, was a minimum at t_1/d of 0.5, and varied little between values of 0.25 and 1.0. Tests with syntactic foam projectiles and an aluminum alloy, two-plate structure indicate, however, that the minimum thickness of the combined plates occurs at values of t_1/d below 0.25 (ref. 40).

Other significant shield characteristics have been established (refs. 21, 32, 38, and 41). In particular, fragment size tends to increase if the thickness of the shield is too large or if the melting temperature of the shield is high. Also, the strength of the shield is generally not effective when projectile velocity is above approximately 4 km/sec. Subject to the melting-point limitation, shields of different materials but with the same mass-per-unit area are expected to be about equally effective.

The penetration resistance of a multiplate structure may be affected by the inclusion of a lightweight, energy-absorbing medium between the plates. Thermal insulation is frequently utilized for this purpose. The energy-absorbing medium reduces the velocity and size of the fragments. Tests have shown that when velocities are in the range of 4 to 7 km/sec, the medium is effective in reducing fragment-impact damage. Unfortunately, it also serves to transmit the pressure pulse, and in this respect the medium may be detrimental. In the low-velocity regime, the medium is ineffective.

Both fibrous material and foam have been tested as energy absorbers (refs. 32 and 42). When these materials were of the same density and at room temperature, they were equally efficient in reducing fragment-impact damage. Fibrous materials transmitted less shock, however, and were less damaged themselves. It was also discovered that a gap between the shield and the energy-absorbing medium significantly reduced the transmission of the pressure pulse. At substantially reduced temperatures, the fibrous materials retained their flexibility and were clearly more efficient as a result. Multisheet thin foils were also tested and found to be ineffective.

Flexible, fibrous materials may be effective in reducing penetration over a limited velocity range. At the higher meteoroid velocities, this material is of questionable benefit and may even be detrimental. Therefore, it is assumed that no benefit will result from the use of an energy-absorbing medium.

The use of conventional honeycomb between the plates of a multiplate structure has also been investigated (refs. 21, 36, 42, and 43). It has been demonstrated both experimentally and analytically that the honeycomb acts to channel the debris, and it apparently decreases the penetration resistance of the structure. The honeycomb itself is also damaged extensively by the debris. Tests of honeycomb with the cells filled with a flexible foam showed no improvement in penetration resistance, and there was a considerable increase in damage to the honeycomb. The use of conventional honeycomb in a multiplate structure is believed to be detrimental from the standpoint of meteoroid penetration, although it may be justified for other reasons.

Some analytical and experimental investigations have been made of a structure consisting of three spaced plates (refs. 21 and 32). For the same overall spacing, it has been determined that three plates offer no advantage over two plates, and may even be detrimental. The capability of the structure to resist penetration does not appear to be strongly affected by the spacing between the second and third plates.

There are no widely accepted methods for analysis of a multiplate structure subject to meteoroid impact. The various damage modes must be evaluated by hypervelocity-impact tests that simulate the actual conditions as closely as possible. Since the nature of the damage modes varies with velocity, considerable caution must be exercised in interpreting these test data and in extrapolating the data to meteoroid velocities.

2.3.4 Laminated Plates

As defined here, a laminated plate is composed of a number of metallic or nonmetallic plates in intimate contact. The laminations may vary in thickness and material, and no limitations are placed on the number or sequence. These laminations may be bonded together by a metallurgical or adhesive bond, or they may not be bonded. Laminated plates may be employed whenever a combination of materials having different physical characteristics is advantageous (e.g., for radiation protection or in lined radiator tubes).

At any interface between two laminations, one component of the impact-induced pressure pulse is reflected, and another component is transmitted through the interface. The size of the reflected component depends to a first approximation on the acoustic-impedance mismatch between the two laminations, where acoustic impedance is defined as the product of the density of the material and its sonic velocity. The transmitted component is subsequently reflected and transmitted at successive interfaces. These multiple reflections and transmissions may either attenuate or increase the pressure pulse, depending on the phase relationship of the various components. The magnitude of the stress level and the likelihood of spall fracture are affected accordingly (ref. 44).

A limited amount of hypervelocity-impact test data is available for laminated plates (refs. 42 and 45). The impact damage to a laminated plate will usually differ from the damage to a homogeneous plate. Typical damage forms are shown in figure 5. Particular notice should be taken of the ability of a ductile lamination to retain detached spall fragments from a preceding lamination. In addition to the direct damage to the laminations, the pressure pulse may fracture an adhesive bond over an appreciable area. Thick, soft bonds have proven less susceptible to this type of damage than thin, hard bonds.

The characteristics of the impact-induced pressure pulse can be determined accurately only by the use of hydrodynamic/strength techniques such as those described in Section 2.2. However, an analytical method is available in which the amplification or attenuation of an elastic wave may be predicted (ref. 44). This method indicates the degree of interaction between the reflected and transmitted components, but it is not directly applicable to the plastic/elastic pulse caused by high-velocity impact.

There is no adequate method for the prediction of the degree and type of damage to a laminated plate. Each specific type of laminated plate must be tested. The test results cannot be extrapolated to other configurations.

2.3.5 Reinforced Plastic Structure

For structural purposes, a reinforced plastic is defined as a plastic matrix containing short fibers, continuous filaments, or fabric. The matrix is limited to high-strength, thermosetting plastics such as epoxies or phenolics. Either metallics or nonmetallics may be used as the reinforcing medium. Filament-wound motor cases and pressure bottles are the most common examples of this type of structure.

Because the ductility of the plastic matrix is usually quite low, reinforced plastics subject to hypervelocity impact tend to respond in a manner similar to brittle homogeneous materials. Behavior of the reinforced plastics is more complicated, in part because of complex multiple reflections of the pressure pulse from elements of the reinforcing medium.

The impact damage frequently includes extensive delamination of the elements of the reinforcing medium and severe spall of both faces of the plate. The impact crater tends to be rough and irregular in shape, and to have small cracks in its surface. Deep cracks through the thickness of the plate may also occur in the vicinity of the crater. For some materials, the damage will increase as the temperature is reduced. Similar damage results from perforation.

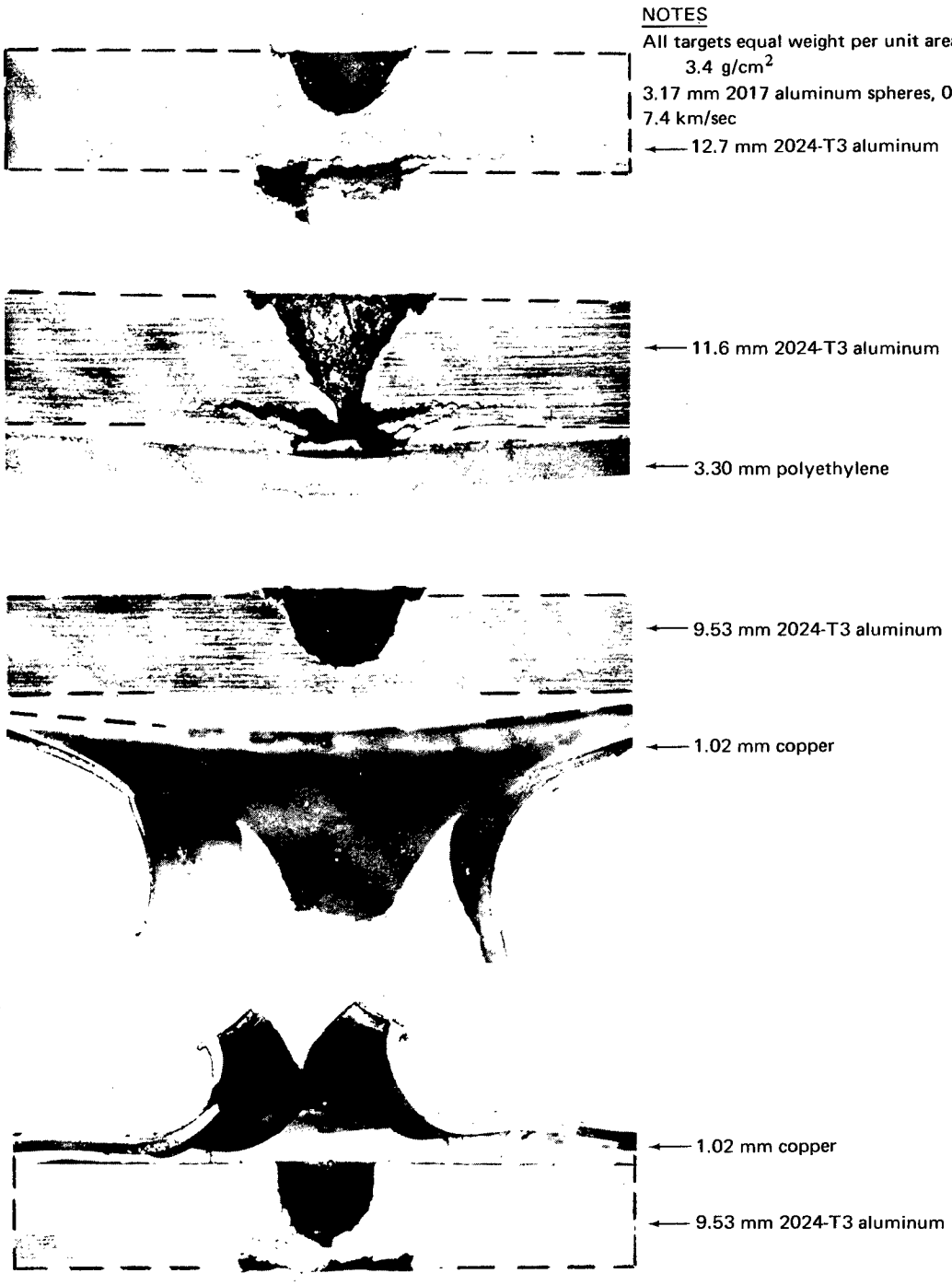

Reproduced by permission of General Motors Defense Research Laboratories

Figure 5. – Effects of laminates on penetration and spall.

No adequate method exists for the prediction of the degree and type of damage to reinforced plastic structures. Each specific type of reinforced plastic structure must be tested. The test results cannot be extrapolated to other configurations.

2.3.6 Subsystems

The previous discussion has been concerned with damage modes common to a number of structural subsystems. Damage modes and concepts peculiar to specific subsystems have also been investigated. The results of these investigations are discussed in the following sections.

2.3.6.1 Pressure Cabins

When the wall of a vessel containing gaseous oxygen is perforated by a projectile, a brilliant flash of light occurs, and this is accompanied by a loud explosion in the interior (ref. 46). The debris from the wall and projectile consists of a cloud of vaporized material and a number of small melted or solid particles (ref. 47). The rapid oxidation of this debris causes the blast. This phenomenon is referred to as vaporific flash.

Vaporific flash is a definite hazard to pressure cabins of space vehicles, particularly if a pure oxygen atmosphere is employed. Secondary fires or injury to the crew can result from either the impact of burning particles projected into the cabin, or from direct contact with the flame.

Combined mechanical and chemical self-sealing concepts have been investigated (ref. 48). For a double-wall structure, it was determined that the outer wall could be sealed satisfactorily within the range of test velocities, but the irregularities of the hole in the inner wall prevented an effective seal. Since the added weight amounted to 4.88 to 7.32 kg/m^2, this concept does not appear attractive. It is probable that onboard detection and repair capability offer a superior approach for manned vehicles.

2.3.6.2 Tanks

Meteoroid damage to tanks may result in leakage, catastrophic rupture, or deflagration. In the event of leakage, the rate is dependent in part on the size and characteristics of the hole in the tank wall. (The characteristics of holes in single and multiplate walls are discussed in Secs. 2.3.2 and 2.3.3, respectively.)

Catastrophic rupture of a tank can be caused solely by the dynamic interaction of the impact damage to the wall with the initial stress field (Secs. 2.3.2 and 2.3.3) or by the

effects of an impact-induced pressure pulse in the tank contents. Analytical and experimental investigations have been made of the causes and characteristics of this pressure pulse (refs. 49 to 51). It has been determined that the pulse is caused by the fluid in the tank when the fluid decelerates the projectile and wall debris, and that the magnitude of the pulse is related to the density and compressibility of the fluid. Consequently, significant pressure pulses are observed only in tanks containing liquids. With gas, the pulse and its effects are negligible (ref. 47).

Perforation of the tank wall results in the formation of a hemispherical shock wave, with its origin at the point of impact. This pressure pulse typically lasts a few microseconds. As an indication of the severity of the shock, pressures as high as 5.17 GN/m^2 have been measured (ref. 52). These pressures are completely attenuated within a few centimeters, with the result that the phenomenon is in most instances independent of tank size.

These local pressures cause additional stress in the tank wall adjacent to the point of impact. The level of these incremental stresses depends both on the magnitude of the shock and on the shape and duration of the pressure pulse. The pressure-induced stress combines with any initial stress in the tank wall and the dynamic stress caused by formation of the hole. When the total exceeds the dynamic fracture strength of the wall material, catastrophic rupture results. The fracture is initiated within the time duration of the pressure pulse (refs. 52 and 53). It should be noted that the projectile velocity at which catastrophic rupture will occur because of the pressure pulse is substantially greater than the velocity causing threshold penetration of the wall, and that there is a minimum velocity below which catastrophic rupture will not occur. Moreover, for projectiles of equal kinetic energy (ref. 50), there are indications that small, low-density projectiles at high velocities are more destructive than larger projectiles at low velocities.

Some experimental data are available on tank penetration (refs. 32 and 51). These data illustrate tank-rupture problems qualitatively, but they are applicable only to the particular cases tested.

Deflagration, or extremely rapid burning, occurs only with certain combinations of tank-wall materials and contents, notably titanium and oxygen. When the wall of a titanium tank containing liquid or gaseous oxygen is perforated by a projectile, deflagration almost always results. In some cases, an explosion may also occur. After ignition, the deflagration will ordinarily be sustained until the titanium or the oxygen is consumed. Tests have demonstrated that both pure titanium and various titanium alloys have approximately the same sensitivity to deflagration. Moreover, coating the titanium with various metals and plastics does not reduce the sensitivity when perforation occurs (refs. 52, 54, and 55).

With other oxidizers, the sensitivity of titanium to deflagration is substantially reduced. Tests with nitrogen tetroxide (N_2O_4) showed no sustained reaction and only minor evidence of local oxidation (ref. 52). Similarly, tests with air at atmospheric pressure showed only an impact flash (ref. 55).

Other tank materials were investigated in conjunction with liquid and gaseous oxygen to determine their sensitivity to deflagration. It was established that magnesium and low-alloy steels were quite sensitive, but that aluminum alloys showed only local oxidation with no sustained reaction. The 300 series (austenitic) stainless steels and nickel alloys were insensitive, and no reaction occurred (refs. 52, 54, and 55).

2.3.6.3 Radiators

Meteoroid damage to radiative surfaces usually has little effect on the function of the radiator, other than long-term erosion of the thermal coatings. However, meteoroid impact on the radiator tubes can cause significant damage. In addition to loss of fluid from perforation of the tube wall, partial penetration can cause deformation or dimpling of the inner surface and consequent restriction of the coolant flow. The coolant fluid can also be contaminated by detached spall fragments with subsequent severe consequences for the various valves and pumps. This latter situation can be alleviated by the addition of a ductile metal liner to retain the spall fragments.

Many materials that are attractive for radiator tubes from the thermal standpoint are quite brittle (e.g., graphite). For such materials, the indirect damage caused by the reflections and interactions of the impact-induced pressure pulse can be particularly severe. Deep cracks through the tube wall can occur both at the point of impact and at more remote locations (ref. 34). Loss of the coolant fluid can be prevented by a ductile metal liner, but the structural strength of the radiator will be impaired.

A limited number of hypervelocity-impact tests have been made on thick-walled radiator tubes with and without ductile metal liners (refs. 34, 35, and 56). From the available experimental data, it appears that small-diameter radiator tubes resist perforation, spall, and dimpling better than larger tubes. However, the amount of data is inadequate to establish specific design methods.

2.3.6.4 Thermal Protection Systems

Ablative and radiative thermal-protection systems will be considered in this section. The radiative systems will be limited to refractory metals, usually with an oxidation-resistant coating.

Ablative systems consist of an ablative element bonded to a metal or plastic substrate. The ablative element is usually a reinforced plastic (e.g., carbon phenolic) or an elastomer which is sometimes used in conjunction with an open-face honeycomb. The honeycomb is bonded to the substrate and its cells are filled with the elastomer.

Hypervelocity impact can result in either partial penetration or perforation of the ablative element. The impact-induced pressure pulse can fracture the bond between the ablative element and the substrate over a substantial area and can cause deformation, backface spall, or fracture of the substrate. With a metal substrate, a large petalled hole frequently occurs. These types of damage can occur without perforation of the ablative element.

The damage to a reinforced-plastic ablative element is similar to that described in Section 2.3.5. In addition to this type of damage, severe cracking may occur in small panels as a result of reflection of the pressure pulse from the edges. In an elastomeric ablative element, the impact crater is frequently quite deep and narrow, even at the highest test velocities. Caution must be exercised in interpreting data on this type of crater, since the crater is not in the hypervelocity regime. When the elastomer is contained by a honeycomb, the apparent damage tends to be more localized, but debonding of the elastomer from the cell walls can occur over a larger area.

The oxidation-resistant coatings that are customarily used with refractory-metal radiative panels tend to be quite brittle. In addition to partial penetration or perforation, and possible cracks through the thickness of the refractory-metal plate, hypervelocity impact can also cause extensive spall damage to the coating on both the front and back faces.

Some experimental impact data are available for ablative thermal-protection systems (refs. 36, 42, and 57). While these data may serve as a guide, they cannot be extrapolated to other configurations.

2.3.6.5 Windows

Simulated meteoroid-impact tests have been conducted on glass windows (refs. 33 and 36). In these tests, the windows were partially penetrated, perforated, or cracked at the point of impact and at the edges. The cracks at the edges were the result of the reflection of the pressure pulse from the edges and it has been demonstrated that the extent of the edge cracks depends on the size of the pane and on the boundary conditions. Cracking and pulverizing at the point of impact can be sufficiently severe to make the immediately surrounding area opaque.

A few tests have been made on windows composed of two glass panes spaced a short distance apart. With the double panes, the integrity of the inner panel could be maintained, provided it was not impacted by debris from the outer panel or projectile.

Some experimental data are available for the impact of unusually small particles on thick glass specimens. While these data serve as a guide to the degree of damage from partial penetration, they do not include the potentially more serious effects of cracking adjacent to the boundaries (ref. 58).

2.3.6.6 Special-Purpose Surfaces

Certain surfaces on a space vehicle (e.g., a solar collector) are required to possess specific optical, thermal, or other special properties. Multiple impacts by meteoroids can cause erosion of these surfaces and consequent degradation of their function. However, the degree of erosion does not necessarily correspond on a one-for-one basis with degradation of the function. Limited tests have been made of this phenomenon (ref. 11).

2.4 Summary

Scattered facts have been accumulated on the subject of protecting spacecraft from meteoroids, but these have not been related to form a coherent body of knowledge. Test results have frequently been cause for revision of theory, rather than confirmation of theory. Estimated characteristics of the meteoroid environment remain to be duplicated in the laboratory, thus hindering the development of basic principles of protection from this environment. In spite of these difficulties, models of the meteoroid environment have been developed, and theoretical and experimental methods have been devised for the design and analysis of meteoroid protection systems for operational spacecraft.

Analytical methods (both theoretical and empirical) are used to estimate the degree of meteoroid damage to simple structural components (i.e., semiinfinite bodies or single plates). Analytical methods are sometimes also used to estimate the damage to more complex structural components. However, tests are always conducted to verify the type and degree of damage expected. Test specimens simulate the actual components as nearly as practicable, and test projectiles simulate kinetic energies expected from meteoroid impacts. Analyses are also made to establish conservatively the probability that a component will fail because of a meteoroid impact. Classical probability theory is then used to estimate the reliability of the space vehicle, considering the meteoroid hazard and all other potential causes of loss of flightworthiness.

3. CRITERIA

The structural design of the space vehicle shall ensure that damage which may result from meteoroids does not constitute an undue hazard to flightworthiness.

3.1 Meteoroid Environment

The potential hazard from meteoroids shall be assessed on the basis of the mission profile and the best available models of the environment.

3.2 Damage Assessment

The degree of structural damage expected from meteoroid impact shall be determined by analysis and applicable experimental data. The damage assessment shall include the types of failure listed in table II and any others which may be pertinent.

3.3 Vehicle Reliability

The required probability that meteoroid damage will not endanger the flightworthiness of the vehicle shall be established, and shall be compatible with the specified overall reliability for the vehicle.

TABLE II. – PROBABLE CRITICAL TYPES OF FAILURE FOR VARIOUS SUBSYSTEMS

Probable critical types of failure	Subsystems					
	Pressure cabins	Tanks	Radiators	Windows	Special-purpose surfaces	Entry thermal protection
Catastrophic rupture	x	x		x		(To be established in terms of the specific thermal protection system.)
Secondary fractures			x			
Leakage	x	x	x			
Vaporific flash	x					
Deflagration		x				
Deformation			x			
Reduced residual strength	x	x	x	x		
Fluid contamination		x	x			
Thermal insulation damage	x	x				
Obscuration				x		
Erosion					x	

3.4 Subsystems Reliability

The minimum probability that each subsystem will not fail because of meteoroid damage shall be established. The combined minimum probability for all subsystems shall not be less than the required probability that meteoroid damage will not endanger flightworthiness of the vehicle.

3.5 Tests

The type and degree of damage to structural subsystems, expected to be caused by meteoroid impact, shall be substantiated by appropriate proof tests.

4. RECOMMENDED PRACTICES

4.1 Meteoroid Environment

Meteoroid flux can consist of three independent components: cometary meteoroids, asteroidal meteoroids, and lunar ejecta. The model meteoroid environment specified in reference 1 covers cometary meteoroids and lunar ejecta, and should be used for near-earth, cis-lunar, and near-lunar missions. For the environment in interplanetary space, and particularly in the asteroidal belt between Mars and Jupiter, a separate NASA monograph is planned. It should be used in conjunction with reference 1 when it becomes available.

The probability of impact by meteoroids should be based on the following Poisson distribution equation:

$$P_{x \leqslant n} = \sum_{r=0}^{r=n} \left[\frac{e^{-NA\tau} (NA\tau)^r}{r!} \right] \qquad (1)$$

where

$P_{x \leqslant n}$ = probability of impact by n meteoroids or less

N = expected flux, particles/m^2 -sec

A = exposed area, m^2

τ = exposure time, sec

The flux used in equation (1) should be adjusted to account for the effects of gravitational defocusing and of shielding of the space vehicle by planetary bodies or by parts of the vehicle itself (ref. 1). The area should be chosen after carefully considering the shape of the space vehicle or part, and the meteoroid environment component being analyzed. When analyzing a component of the environment having an omnidirectional flux, the surface area of the vehicle or part should be used. When considering a component having a directional flux, the projected area perpendicular to the flux stream should be used.

With the equation and the mass-flux relations of reference 1, the probability of impact by n or less meteoroids of a particular mass or greater should be established.

4.2 Damage Assessment

4.2.1 Methodology for a Semiinfinite Body

In some single-wall structures, it is desirable to limit the depth of penetration to a small fraction of the plate thickness. If this limit is 25 percent or less, the plate may be considered semiinfinite. Under this condition, the following empirical equation for depth of penetration, adapted from references 24 and 26, is recommended for design:

$$P_{\infty} = K_{\infty} m^{0.352} \rho_m^{\frac{1}{6}} V^{\frac{2}{3}} \qquad (2)$$

where

P_{∞} = depth of penetration, cm

K_{∞} = a constant

m = mass of meteoroid, g

ρ_m = density of meteoroid, g/cc

V = impact velocity, km/sec

The constant K_{∞} is a characteristic of the target material and its temperature. Known values of this constant are tabulated in table III. For other materials and conditions, its value must be determined by hypervelocity-impact tests which duplicate the specific structural parameters.

TABLE III. – CONSTANTS FOR CRATER DEPTH IN A SEMIINFINITE BODY (ROOM TEMPERATURE)

Material	K_∞
Aluminum alloys	
2024-T3, -T4	0.42
2014-T6	
7075-T6	
6061-T6	
Stainless steel	
AISI 304	0.25
AISI 316	

Equation (2) is considered satisfactory for the anticipated range of meteoroid mass and density. The dependence on velocity was established from experimental data obtained at velocities of 8 km/sec or less. It is believed to be somewhat conservative at the higher meteoroid velocities. The equation is primarily for ductile structural metals; it is of doubtful value for low-ductility metals and is generally unsuitable for nonmetals.

To determine the extent of surface area destroyed it is necessary to rely on hypervelocity impact tests.

4.2.2 Methodology for Thin Plates

The following empirical equation, adapted from reference 59, is recommended for design to establish the threshold penetration of a thin, ductile, metal plate:

$$t = K_1 m^{0.352} \rho_m^{\frac{1}{6}} V^{0.875} \qquad (3)$$

where

t = thickness of plate penetrated, cm

K_1 = a constant

m = mass of the meteoroid, g

ρ_m = density of the meteoroid, g/cc

V = impact velocity, km/sec

The thickness required to prevent spall or deformation of the back surface will be appreciably larger than the thickness determined by this equation. Some experimental evidence indicates that the equation may result in an overestimation of the thickness required to prevent threshold penetration of metal films a few hundredths of a millimeter thick.

The constant K_1 is a characteristic of the target material and its temperature. Known values of this constant are tabulated in table IV in conjunction with the basis by which threshold penetration was measured. It is important that the basis for K_1 be consistent with the requirements of the particular structure in question.

The occurrence of incipient spall can be estimated (ref. 21), but quantitative relationships are not available for the prediction of detached spall. For detached spall, the spall thickness will frequently range from 1/10 to 1/2 the plate thickness, and the diameter of the spalled area from two to three times the plate thickness.

The following empirical equation is recommended as a first approximation of the clear-hole diameter in thin, ductile metal plates (ref. 60):

$$\frac{D}{d} = 0.45\left(\frac{t}{d}\right)^{\frac{2}{3}} V + 0.90 \qquad (4)$$

where

D = clear-hole diameter

d = diameter of the meteoroid

t = thickness of the plate

V = impact velocity, km/sec

TABLE IV. – CONSTANTS FOR THRESHOLD PENETRATION OF A SINGLE PLATE (ROOM TEMPERATURE)

Material	K_1	Basis
Aluminum alloys		
2024-T3, -T4	0.54	Visual
7075-T6	0.57	Pressure
6061-T6		
Stainless steels		
AISI 304	0.32	Pressure
AISI 316		
17 – 4 PH annealed	0.38	Pressure
Magnesium lithium		
LA 141-A	0.80	Pressure
Columbium alloys		
Cb - 1Zr	0.34	Pressure

This equation is limited to plates that are perforated with an approximately cylindrical hole, as shown in figure 2. Consequently, the meteoroid mass required for the clear-hole perforation will be somewhat larger than the meteoroid mass applicable to threshold penetration. For aluminum and steel projectiles, this equation agrees well with experimental data. However, for frangible projectiles (e.g., pyrex glass or syntactic foam), there is some experimental evidence which indicates it is slightly conservative (refs. 21 and 37). The strength and density of the plate material also have a minor effect (ref. 60).

Equations (3) and (4) are both recommended for the anticipated range of meteoroid mass and density. The velocity dependence of both equations is based on experimental data obtained at velocities of 8 km/sec or lower. Extrapolation of these equations to the higher meteoroid velocities is believed to yield acceptable results, but may be slightly conservative. These equations are valid only for impact normal to the surface and are generally limited to ductile structural metals. They are of doubtful value for low-ductility metals and are unsuitable for nonmetals.

For materials, conditions, and damage modes other than those for which data are presented here, it is necessary to rely entirely on hypervelocity-impact tests which duplicate the specific structural factors.

4.2.3 Methodology for Subsystems

4.2.3.1 Pressure Cabins

Single-wall pressure cabins should be treated as gas-filled tanks. The following considerations apply to pressure cabins of multiwall construction (i.e., two or more spaced plates). The required wall thickness should be determined by suitable tests. Penetration tests should be conducted over a velocity range which includes the low-velocity peak and extends to at least 7.5 km/sec (fig. 3).

When a cabin wall is perforated by a meteoroid, failure can occur because of loss of the cabin atmosphere. The degree of failure can range from an instantaneous complete failure in the case of rapid decompression to a delayed complete failure at more moderate leakage rates. Inflight detection and repair capability should be considered as a means of limiting moderate leakage rates to partial failure. The leakage rate is determined primarily by the cabin pressure and the size and condition of the hole. These hole characteristics should be determined by test for holes in the second and in any subsequent plates. In some cases, the size and condition of the hole in the outer plate will govern the leakage rate. For a thin ductile-metal outer plate, equation (4) should be used to estimate the hole diameter.

Insulation is frequently installed between the inner and outer plates of a pressure cabin wall to provide thermal control. For a thin ductile-metal outer wall, equation (3) should be used to estimate the minimum mass of a meteoroid capable of threshold penetration. An impact by a meteoroid of larger mass will destroy the insulation around the point of impact and cause degradation of the thermal control. The extent of this destruction should be determined by test.

The type and degree of failure resulting from vaporific flash, catastrophic rupture, or reduced residual strength should be evaluated by test. The actual cabin atmosphere and pressure should be duplicated for vaporific-flash tests. Sufficient volume should be provided to allow the cone of flame to develop as it would in the actual cabin, with sufficient oxygen provided to prevent premature depletion.

4.2.3.2 Tanks

The following recommendations are for design of single-wall tanks that are directly exposed to meteoroid impact. For gas- or liquid-filled tanks at high stress levels, experimental data indicate that the depth of penetration should not exceed 25 percent of the tank-wall thickness. Equation (2) should be used to estimate the depth of penetration. For liquid-filled tanks at low stress levels, the depth of penetration should be limited to the amount that would cause threshold penetration of the tank wall. Equation (3) should be used to estimate threshold penetration of the tank wall. To assess leakage, equation (4) should be used to estimate the hole diameter. Deflagration should be eliminated by the proper choice of materials. Except for deflagration tests, specimens simulating liquid-filled tanks should use either the actual fluid or one of equal density and compressibility, pressurized to the same level as the actual tank. For gas-filled tanks, only the static stress level is significant. For deflagration tests, the actual liquid or gas should be used. For the design of double-wall tanks or for single-wall tanks shielded by other structure, the type and degree of failure should also be determined by test.

4.2.3.3 Radiators

The degree of radiator failure resulting from meteoroid impact depends strongly on the design and redundancy of the specific radiator subsystem. The type and degree of failure should be substantiated by test. If the coolant fluid is a liquid, the test specimen should contain either the actual liquid or one of equal density and compressibility, and at the same pressure as the actual liquid.

4.2.3.4 Thermal Protection Systems

Thermal protection systems should be tested to determine the type and degree of possible meteoroid damage and to determine whether this damage will cause failure of the protective function. For the panels in the thermal protection system where edge effects may be significant, the test specimen should be full size. Thermal tests should be conducted to determine the effect of meteoroid damage on the thermal protection system.

4.2.3.5 Windows

The type and degree of window failure should be determined by test, including small-particle impact tests and thermal tests. The test specimens should be full size and the edge-support conditions should be duplicated.

4.2.3.6 Special-Purpose Surfaces

Erosion of special-purpose surfaces should be evaluated by multiple impact tests which relate the degree of surface damage to the degree of degradation of the function. The type of test described in reference 11 is suitable for special-purpose surfaces when used in conjunction with the meteoroid environment of reference 1.

4.3 Vehicle Reliability

For each spacecraft, a level of reliability is required in the vehicle specifications. Since meteoroids are one of the several conditions involved in flight, a separate required probability value should be established that meteoroid damage will not endanger the flightworthiness of the vehicle. The recommended procedure for analysis of meteoroid damage and determination of the flightworthiness of the vehicle is outlined in figure 6.

4.4 Subsystems Reliability

The probability that meteoroid damage will not endanger the flightworthiness of each subsystem should be determined. If a subsystem can just withstand without failure the impact of n or less meteoroids of mass m or greater, $P_{x \leqslant n}$ becomes the probability that failure – that is, the loss of subsystem flightworthiness – will not occur.

The probability of "no failure" for exposure to more than one component of the meteoroid flux should be obtained by the conventional combined probability relations for independent events. Similarly, the combined probability of no failure for the vehicle as a whole should be determined from the probability of no failure for the various subsystems.

Meteoroid damage from a single impact may cause either complete or partial failure of a subsystem. Complete failure may be instantaneous, as in catastrophic rupture; or delayed, as in the leakage of a pressure-cabin atmosphere. Partial failure implies degradation of the subsystem, but not destruction of its flightworthiness. Multiple impacts, however, may cause sufficient cumulative damage to result in a delayed complete failure. For example, failure can result from cumulative damage to the thermal insulation of a pressure cabin or from erosion of an optical surface. The degree of damage necessary to cause each type of failure is not necessarily the same, and consequently the probability of nonoccurrence will differ.

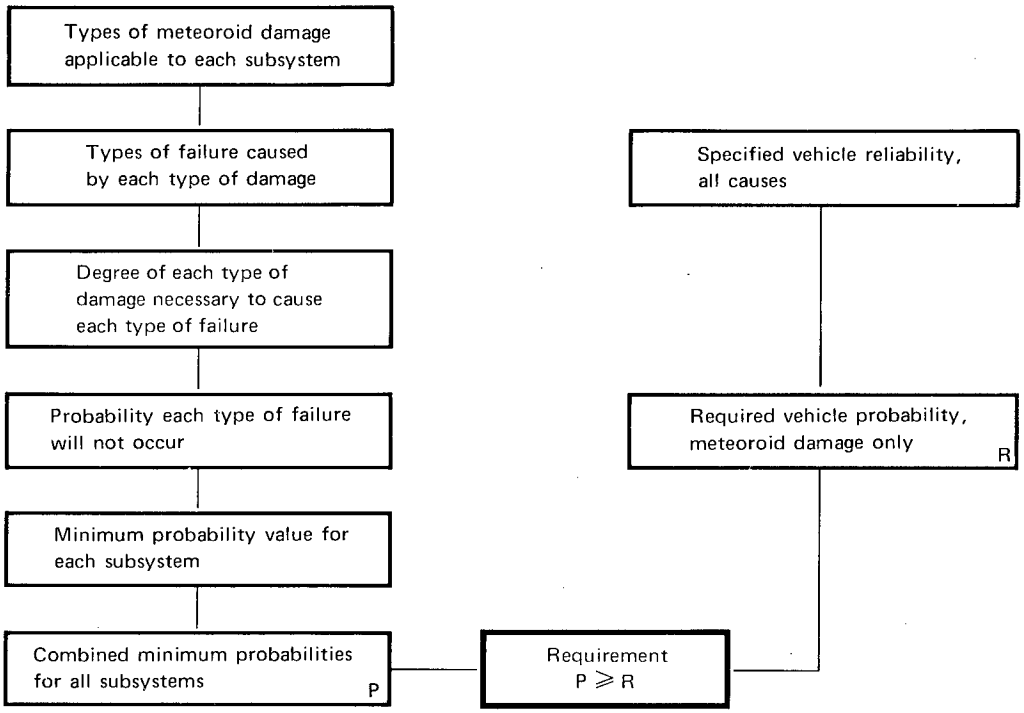

Figure 6. – Procedure for analysis of meteoroid damage and determination of flightworthiness.

For each subsystem and each type of damage, the degree of damage necessary to cause any applicable type of failure of the subsystem should be determined. The probability that this degree of damage will not occur should be determined for each type of failure, and the minimum probability value established for the subsystem. If the minimum predicted probability is unacceptable, the subsystem configuration must be modified to increase its resistance, or a reduction must be justified in the specified probability.

4.5 Tests

Meteoroid-impact tests involve two phases: development and proof tests. The final design of all structural subsystems that could fail because of meteoroid impact and endanger the vehicle's flightworthiness should be substantiated by proof tests. In addition, where analytical relationships are not available, development tests should be conducted for design purposes. The following considerations are applicable to both phases of testing.

The meteoroid should be simulated preferably by either a sphere or a cylinder with approximately equal dimensions. Aluminum and glass are satisfactory materials to use in simulating stony meteoroids. The above materials and syntactic foam are acceptable

for the simulation of low-density cometary meteoroids. For high-density asteroidal meteoroids, steel is satisfactory.

A light-gas gun is recommended as the particle accelerator. Because this device cannot achieve the velocities required for cometary or asteroidal meteoroids, velocity scaling is necessary. Where a mass-velocity-density relationship has been established [e.g. eqs. (2) to (4)], velocity scaling should be based on this relationship; otherwise, the velocity should be scaled on the basis of equal kinetic energy. Test velocities should extend to at least 7.5 km/sec. Because lunar ejecta have much lower velocities than cometary or asteroidal meteoroids, and do not exceed the velocity capability of light-gas guns, the velocity of the test particles should duplicate that of the lunar ejecta.

The test specimens should duplicate the geometry, material, temperature, and stress level of the structural subsystem under consideration. Geometrical scaling of the specimen is not recommended. However, with certain exceptions, it is not necessary to duplicate the area or volume of the subsystem. The test specimen need only be of sufficient size to avoid edge effects.

Special considerations applicable to particular subsystems are discussed in Section 4.2.3.

REFERENCES

1. Anon: Meteoroid Environment Model – 1969 [Near Earth to Lunar Surface]. NASA Space Vehicle Design Criteria (Environment), NASA SP-8013, 1969.

2. Zimmerman, F. J.; et al.: Proceedings of the Sixth Hypervelocity Impact Symposium. Vol. I, Aug. 1963.

3. Charters, A. C.; et al.: Proceedings of the Seventh Hypervelocity Impact Symposium. Vol. I, Feb. 1965.

4. Denardo, B. Pat: Penetration of Polyethylene into Semi-Infinite 2024-T351 Aluminum up to Velocities of 37,000 Feet per Second. NASA TN D-3369, 1966.

5. Moore, E. T.: Explosive Hypervelocity Launchers. NASA CR-982, 1968.

6. Scully, C. N.; et al.: Electrothermal Gun for Hypervelocity Ballistics Research. Proceedings of the Seventh Hypervelocity Impact Symposium. Vol. I, Feb. 1965.

7. Friichtenicht, J. F.; et al.: Electrostatic Accelerators – Experimental Techniques. Proceedings of the Seventh Hypervelocity Impact Symposium. Vol. I, Feb. 1965.

8. Myrberg, John E.; and Clark, William H.: Development of Hypervelocity Guns Using a Capacitive Energy Source. Tech. Rept. AFML-TR-66-252, Air Force Materials Laboratory, Sept. 1966.

9. Alfaro-Bou, E.; and Thomson, R. G.: Ballistic Limit of Aluminum Plates Determined by an Exploding Foil Gun Technique. NASA TN D-4259, 1967.

10. Carlson, R. E.; and Fager, J. A.: Effects of Hypervelocity Impact on Semi-Infinite Plate and Composite Spacecraft Hulls from 18,000 fps to 100,000 fps. AIAA Sixth Structures and Materials Conference, (Palm Springs Calif.) Apr. 5-7, 1965.

11. Mirtich, M. J.; and Mark, Herman: Feasibility of Accelerating Micron-Size Particles in Shock-Tube Flows for Hypervelocity Degradation of Reflective Surfaces. NASA TN D-3187, 1966.

12. Bjork, R. L.; et al.: Analytical Study of Impact Effects as Applied to the Meteoroid Hazard. NASA CR-757, 1967.

13. Walsh, J. M.; and Johnson, W. E.: On the Theory of Hypervelocity Impact. Proceedings of the Seventh Hypervelocity Impact Symposium. Vol. II, Feb. 1965.

14. Riney, T. D.; and Heyda, J. F.: Hypervelocity Impact Calculations. Proceedings of the Seventh Hypervelocity Impact Symposium. Vol. II, Feb. 1965.

15. Bjork, R. L.: Review of Physical Processes in Hypervelocity Impact and Penetration. Proceedings of the Sixth Hypervelocity Impact Symposium. Vol. II, Part 1, Aug. 1963.

16. Read, H. E.; and Bjork, R. L.: A Numerical Study of the Hypervelocity Impact of a Cylindrical Projectile with a Semi-infinite Target. Rept. SH-8235 F, Shock Hydrodynamics, Inc., Aug. 1967.

17. Dienes, J. K.; and Evans, M. W.: Cratering Calculations with a Hydrodynamic Strength Code. Rept. GA-8071, Gulf General Atomic, Inc., 1967.

18. Rosenblatt, M.; et al.: Analytical Study of Debris Clouds Formed by Hypervelocity Impacts on Thin Plates. Rept. SH-2015 F, Shock Hydrodynamics, Inc., Aug. 1968.

19. Tillotson, J. H.: A Theoretical and Experimental Correlation of Hypervelocity Impact on Layered Targets. Tech. Rept. S-425-R, Edgerton, Germeshausen and Grier, Inc., May 1968.

20. Kreyenhagen, K. N.; et al.: Numerical Solution of Oblique Impacts. Proceedings of the Seventh Hypervelocity Impact Symposium. Vol. III, Feb. 1965.

21. McMillan, A. R.: Experimental Investigations of Simulated Meteoroid Damage to Various Spacecraft Structures. NASA CR-915, 1968.

22. Madden, Richard: Ballistic Limit of Double-Walled Meteoroid Bumper Systems. NASA TN D-3916, 1967.

23. Thomson, R. G.: Analysis of Hypervelocity Perforation of a Visco-Plastic Solid Including the Effects of Target-Material Yield Strength. NASA TR R-221, 1965.

24. Summers, James L.: Investigation of High-Speed Impact: Regions of Impact and Impact at Oblique Angles. NASA TN D-94, 1959.

25. Christman, D. R.; et al.: Summary Report – Study of the Phenomena of Hypervelocity Impact. Rept. TR 63-216, General Motors Defense Research Laboratories, June 1963.

26. Denardo, B. Pat; et al.: Projectile Size Effects on Hypervelocity Impact Craters in Aluminum. NASA TN D-4067, 1967.

27. Halperson, S. M.: Comparisons Between Hydrodynamic Theory and Impact Experiments. Proceedings of the Seventh Hypervelocity Impact Symposium. Vol. V, Feb. 1965.

28. Herrman, W.; and Jones, A. H.: Survey of Hypervelocity Information. A.S.R.L. Rept. 99-1, Lincoln Laboratory, Massachusetts Inst. of Technol., Sept. 1961.

29. Piacesi, R.; et al.: Determination of the Yield Strength as an Effective Mechanical Strength Property in the Cratering Process of Hypervelocity Impact. Proceedings of the Seventh Hypervelocity Impact Symposium. Vol. V. Feb. 1965.

30. Bruce, E. P.: Hypervelocity Impact of Single Thin Sheet Structures – Incipient Perforation Conditions. Proceedings of the Seventh Hypervelocity Impact Symposium. Vol. VI. Feb. 1965.

31. Halperson, S. M.: Some Phenomena Associated with Impacts Into Aluminum. Proceedings of the Sixth Hypervelocity Impact Symposium. Vol. II, Part 2, Aug. 1963.

32. Lundeberg, J. F.; et al.: Meteoroid Protection for Spacecraft Structures. NASA CR-54201, 1965.

33. Diedrich, James H.; and Stepka, Francis S.: Investigation of Damage to Brittle Materials by Impact with High Velocity Projectiles into Glass and Lucite. NASA TN D-2720, 1965.

34. Diedrich, James H.; et al.: Hypervelocity Impact Damage Characteristics in Beryllium and Graphite Plates and Tubes. NASA TN D-3018, 1965.

35. McMillan, A. R.: Hypervelocity Impacts Into Stainless-Steel Tubes Armored with Reinforced Beryllium. NASA TN D-3512, 1966.

36. Gehring, J. W.; et al.: Final Report on Hypervelocity Impact Studies Against Apollo-Type Structures up to 16.5 km/sec. Rept. TR 65-56, General Motors Defense Research Laboratories, July 1965.

37. Nysmith, C. Robert; and Summer, James L.: An Experimental Investigation of the Impact Resistance of Double Sheet Structures at Velocities to 24,000 Feet Per Second. NASA TN D-1431, 1962.

38. Maiden, C. J.; et al.: Thin Sheet Impact. Proceedings of the Seventh Hypervelocity Impact Symposium. Vol. IV, Feb. 1965.

39. Swift, H. F.; and Carson, J. M.: Ballistic Limits of 6061-T6 Aluminum Bumper Systems. Rept. AFML-TR-67-324, Air Force Materials Laboratory, Oct. 1967.

40. Teng, R. N.: Hypervelocity Impact Damage in Aluminum Targets: Final Report. Rept. DAC-59816, Douglas Aircraft Co., Feb. 1968, rev. Mar. 1968.

41. Swift, H. F.; and Hopkins, A. K.: The Effects of Bumper Material Properties on the Operation of Spaced Hypervelocity Particle Shields. Rept. AFML-TR-68-257, Air Force Materials Laboratory, Sept. 1968.

42. Summers, J. L.; and Nysmith, C. R.: The Resistance of a Variety of Composite Space Structures to Hypervelocity Impact. AIAA, Fifth Structures and Materials Conference (Palm Springs, Calif.), Apr. 1-3 1964.

43. Gehring, J. W.; et al.: Final Report on The Effects of Hypervelocity Impact on Structures Representative of the Apollo Service Module. Rept. TR 68-04, AC Electronics – Defense Research Laboratories, Dec. 1967.

44. Kinslow, Ray: Stress Waves in Composite Laminates. Rept. AEDC-TR-65-69, Air Force Systems Command, June 1965.

45. McMillan, A. R.: An Investigation of the Penetration of Hypervelocity Projectiles into Composite Laminates. Proceedings of the Sixth Hypervelocity Impact Symposium. Vol. III, Aug. 1963.

46. Gehring, John W.; et al.: Spacecraft Interior Hazards from Hypervelocity Impact. Rept. TR-66-13, General Motors Defense Research Laboratories, Mar. 1966.

47. Friend, W. H.; et al.: An Investigation of Explosive Oxidations Initiated by Hypervelocity Impacts. Rept. AFFDL-TR-67-92, Air Force Flight Dynamics Laboratory, Aug. 1967.

48. D'Anna, Philip J.; and Heitz, Roger M.: Evaluation of Self-Sealing Structures for Space Vehicles. NASA CR-485, 1966.

49. Chou, Pei Chi; et al.: Analytical Study of the Fracture of Liquid Filled Tanks by Hypervelocity Particles. NASA CR-72169, 1967.

50. Stepka, Francis S.; et al.: Investigation of Characteristics of Pressure Waves Generated in Water Filled Tanks Impacted by High Velocity Projectiles. NASA TN D-3143, 1965.

51. Ferguson, C. W.: Hypervelocity Impact Effects on Liquid Hydrogen Tanks. NASA CR-54852, 1966.

52. Stepka, Francis S.; et al.: Investigation of Catastrophic Fracturing and Chemical Reactivity of Liquid-Filled Tanks When Impacted by Projectiles of High Velocity. Proceedings of the Seventh Hypervelocity Impact Symposium. Vol. VI, Feb. 1965.

53. Morse, C. Robert; and Stepka, Francis S.: Effect of Projectile Size and Material on Impact Fracture of Walls of Liquid Filled Tanks. NASA TN D-3627, 1966.

54. White, E. L.; and Ward, J. J.: Ignition of Metals in Oxygen. DMIC Rept. 224, Battelle Memorial Institute, Feb. 1, 1966.

55. Riehl, W. A.; et al.: Reactivity of Titanium with Oxygen. NASA TR R-180, 1963.

56. Lieblein, Seymour; and Clough, Nestor: Hypervelocity Impact Damage Characteristics in Armored Space Radiator Tubes. NASA TN D-2472, 1964.

57. McMath, R. R.; et al.: Study of Meteoroid Impact into Ablative Heat Shield Materials. Rept. AVSSD-0002-66-RR, AVCO Corp., Research and Technology Laboratories, Space System Division, Apr. 1966.

58. Posever, F. C.; and Scully, C. N.: Investigation of Structural Implications of Meteoroid Impact. Rept. AFFDL TDR 64-96, Air Force Flight Dynamics Laboratory, July 1964.

59. Fish, Richard H.; and Summers, James L.: The Effect of Material Properties on Threshold Penetration. Proceedings of the Seventh Hypervelocity Impact Symposium. Vol. VI, Feb. 1965.

60. Maiden, C. J.; et al.: Damage to Thin Targets by Hypervelocity Projectiles. Rept. TR 63-225, General Motors Defense Research Laboratories, May 1964.

NASA SPACE VEHICLE DESIGN CRITERIA MONOGRAPHS ISSUED TO DATE

SP-8001	(Structures)	Buffeting During Launch and Exit, May 1964
SP-8002	(Structures)	Flight-Loads Measurements During Launch and Exit, December 1964
SP-8003	(Structures)	Flutter, Buzz, and Divergence, July 1964
SP-8004	(Structures)	Panel Flutter, May 1965
SP-8005	(Environment)	Solar Electromagnetic Radiation, June 1965
SP-8006	(Structures)	Local Steady Aerodynamic Loads During Launch and Exit, May 1965
SP-8007	(Structures)	Buckling of Thin-Walled Circular Cylinders, September 1965 Revised August 1968
SP-8008	(Structures)	Prelaunch Ground Wind Loads, November 1965
SP-8009	(Structures)	Propellant Slosh Loads, August 1968
SP-8010	(Environment)	Models of Mars Atmosphere (1967), May 1968
SP-8011	(Environment)	Models of Venus Atmosphere (1968), December 1968
SP-8012	(Structures)	Natural Vibration Modal Analysis, September 1968
SP-8013	(Environment)	Meteoroid Environment Model – 1969 [Near Earth to Lunar Surface], March 1969
SP-8014	(Structures)	Entry Thermal Protection, August 1968
SP-8015	(Guidance and Control)	Guidance and Navigation for Entry Vehicles, November 1968
SP-8016	(Guidance and Control)	Effects of Structural Flexibility on Spacecraft Control Systems, April 1969
SP-8017	(Environment)	Magnetic Fields – Earth and Extraterrestrial, March 1969
SP-8018	(Guidance and Control)	Spacecraft Magnetic Torques, March 1969
SP-8019	(Structures)	Buckling of Thin-Walled Truncated Cones, September 1968
SP-8020	(Environment)	Mars Surface Models [1968], May 1969
SP-8021	(Environment)	Models of Earth's Atmosphere (120 to 1000 km), May 1969
SP-8023	(Environment)	Lunar Surface Models, May 1969
SP-8024	(Guidance and Control)	Spacecraft Gravitational Torques, May 1969
SP-8025	(Chemical Propulsion)	Solid Rocket Motor Metal Cases, April 1970

SP-8026	(Guidance and Control)	Spacecraft Star Trackers, July 1970
SP-8027	(Guidance and Control)	Spacecraft Radiation Torques, October 1969
SP-8028	(Guidance and Control)	Entry Vehicle Control, November 1969
SP-8029	(Structures)	Aerodynamic and Rocket-Exhaust Heating During Launch and Ascent, May 1969
SP-8031	(Structures)	Slosh Suppression, May 1969
SP-8032	(Structures)	Buckling of Thin-Walled Doubly Curved Shells, August 1969
SP-8033	(Guidance and Control)	Spacecraft Earth Horizon Sensors, December 1969
SP-8034	(Guidance and Control)	Spacecraft Mass Expulsion Torques, December 1969
SP-8035	(Structures)	Wind Loads During Ascent, June 1970
SP-8036	(Guidance and Control)	Effects of Structural Flexibility on Launch Vehicle Control Systems, February 1970
SP-8037	(Environment)	Assessment and Control of Spacecraft Magnetic Fields, September 1970
SP-8038	(Environment)	Meteoroid Environment Model – 1970 (Interplanetary and Planetary), October 1970
SP-8040	(Structures)	Fracture Control of Metallic Pressure Vessels, May 1970
SP-8046	(Structures)	Landing Impact Attenuation for Nonsurface-Planing Landers, April 1970

NASA-Langley, 1971 —— 32